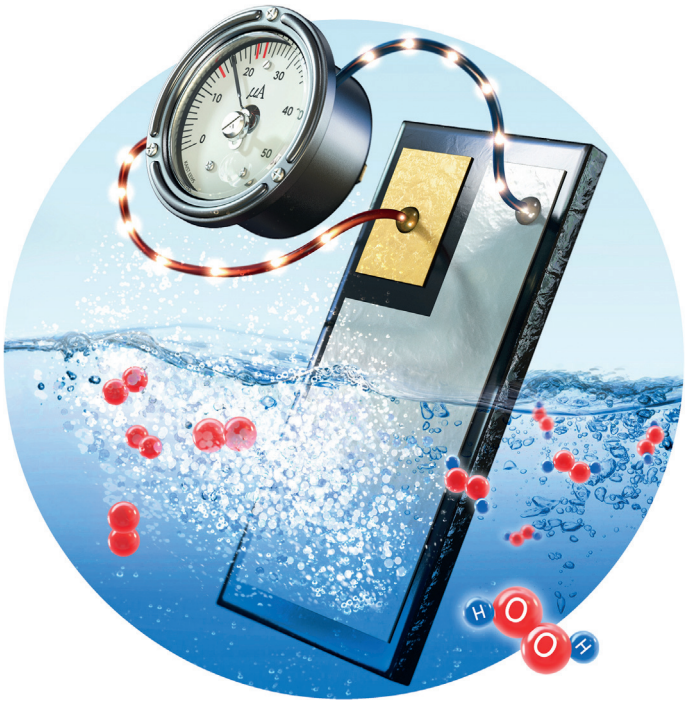

... is expected to be a general phenomenon in exothermic chemical reactions at the gas/solid and solid/liquid interface. In their Communication on page 10859 ff., J. Y. Park and co-workers demonstrate the detection of hot electrons as a chemicurrent generated at the solid/liquid interface during the decomposition of hydrogen peroxide catalyzed on Schottky nanodiodes, and show that the chemicurrent yield can reach values of up to 1/10 electrons per $O_2$ molecule.

***Femtochemistry***

In their Communication on page 10600 ff., E. T. J. Nibbering, T. Elsaesser, and co-workers analyze the Zundel cation by ultrafast pump-probe infrared spectroscopy.

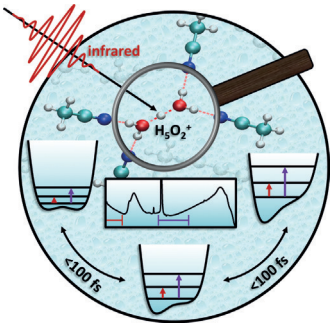


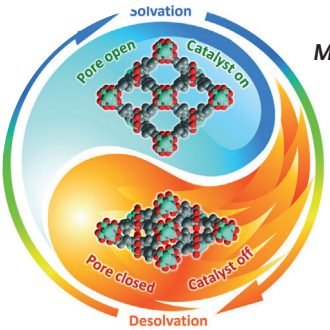


***MOF Catalysts***

Switchable catalysts are prepared by W. Lu, M. B. Hall, H.-C. Zhou, and co-workers in their Communication on page 10776 ff. They show that the catalytic properties of the metal–organic frameworks (MOFs) are controlled by reversible pore opening and closing.

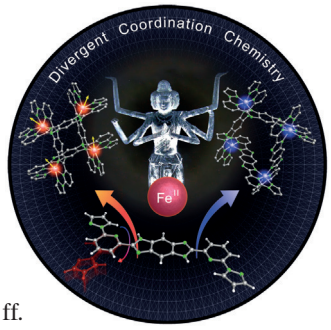


***Divergent Coordination Chemistry***

The coordination of $Fe^{II}$ ions by a homoditopic ligand yields two tauto-isomeric complexes with different magnetic properties. This tautomerism-driven emergence of complexity is explained by M. Ruben et al. in their Communication on page 10881 ff.

## How to contact us:

***Editorial Office:***
*E-mail:* angewandte@wiley-vch.de
*Fax:* (+49) 62 01–606-331
*Telephone:* (+49) 62 01–606-315

***Reprints, E-Prints, Posters, Calendars:***
Carmen Leitner
*E-mail:* chem-reprints@wiley-vch.de
*Fax:* (+49) 62 01–606-331
*Telephone:* (+49) 62 01–606-327

***Copyright Permission:***
Bettina Loycke
*E-mail:* rights-and-licences@wiley-vch.de
*Fax:* (+49) 62 01–606-332
*Telephone:* (+49) 62 01–606-280

***Online Open:***
Margitta Schmitt
*E-mail:* angewandte@wiley-vch.de
*Fax:* (+49) 62 01–606-331
*Telephone:* (+49) 62 01–606-315

***Subscriptions:***
www.wileycustomerhelp.com
*Fax:* (+49) 62 01–606-184
*Telephone:* 0800 1800536 (Germany only)
+44(0) 1865476721 (all other countries)

***Advertising:***
Marion Schulz
*E-mail:* mschulz@wiley-vch.de
*Fax:* (+49) 62 01–606-550
*Telephone:* (+49) 62 01–606-565

***Courier Services:***
Boschstrasse 12, 69469 Weinheim

***Regular Mail:***
Postfach 101161, 69451 Weinheim

*Angewandte Chemie International Edition* is a journal of the Gesellschaft Deutscher Chemiker (GDCh), the largest chemistry-related scientific society in continental Europe. Information on the various activities and services of the GDCh, for example, cheaper subscription to *Angewandte Chemie International Edition*, as well as applications for membership can be found at **www.gdch.de** or can be requested from GDCh, Postfach 900440, D-60444 Frankfurt am Main, Germany.

GDCh
Gesellschaft Deutscher Chemiker

## Service



## Author Profile



*"My favorite author (fiction) is Shiono Nanami. My favorite pieces of music are The Phantom of the Opera and Mozart's Requiem. …"*
This and more about Young-Tae Chang can be found on page 10554.

## News




T. Magauer


O. García Mancheño

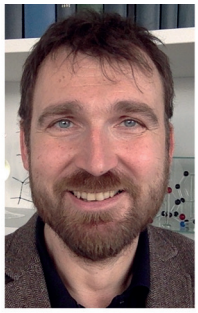
D. Trauner

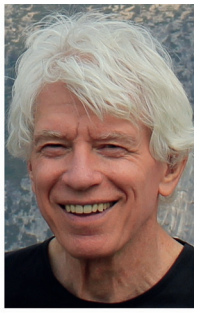
J. P. Richmond

# Highlights

## C–H Arylation



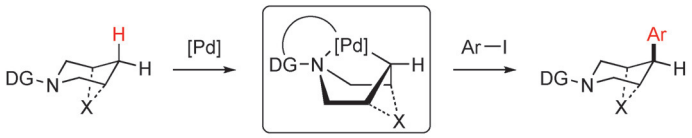


*Transannular C–H activation*

**Now within reach**: In the remote C–H arylation of alicyclic amines the key step is the transannular coordination of the palladium catalyst (see picture, DG = directing group). This strategy is convenient for the late-stage functionalization of complex bioactive molecules in order to probe structure–activity relationships.

# Minireviews

## Beryllium



**Be prepared**: This Minireview presents an introduction to beryllium chemistry. Its toxicity, and that of its compounds, is put into perspective, and safe handling practices are presented. Observations demonstrating the unique chemistry of beryllium and its industrial use are shown and future challenges identified. The picture shows Be metal under Ar in a glass ampule. Picture: A. Heddergott.

# Reviews

## Directing Groups



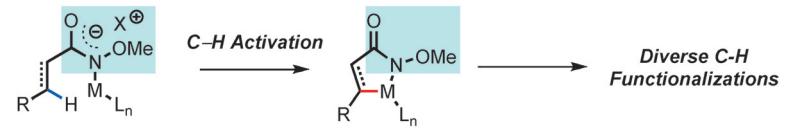


X = Na, K, Cs etc.
M = $Pd^{II}$, $Rh^{III}$, $Ru^{II}$

**Clear directions**: The simple *N*-methoxy amide moiety is a versatile directing group for a wide range of C–H functionalization reactions using Pd, Rh, and Ru catalysis. Whereas it was initially used for Pd-catalyzed C–H activation, it has also been employed in $Rh^{III}$-catalyzed variants and in combination with cheaper ruthenium catalysts.

**For the USA and Canada:**
ANGEWANDTE CHEMIE International Edition (ISSN 1433-7851) is published weekly by Wiley-VCH, PO Box 101161, 69451 Weinheim, Germany. US mailing agent: SPP, PO Box 437, Emigsville, PA 17318. Periodicals postage paid at Emigsville, PA. US POSTMASTER: send address changes to *Angewandte Chemie*, John Wiley & Sons Inc., C/O The Sheridan Press, PO Box 465, Hanover, PA 17331. Annual subscription price for institutions: US$ 16.862/14.051 (valid for print and electronic / print or electronic delivery); for individuals who are personal members of a national chemical society prices are available on request. Postage and handling charges included. All prices are subject to local VAT/sales tax.

  

# Communications

**The Zundel continuum**: Transient infrared pump-probe spectra of the Zundel cation $H_5O_2^+$ dissect OH stretching and bending vibrations from the underlying broadband absorption. The Zundel continuum originates from an ultrafast frequency modulation of the $H^+$ transfer vibration and its combination and overtones by fluctuating electrical interactions with the solvent and stochastic thermal excitations of low-frequency modes.

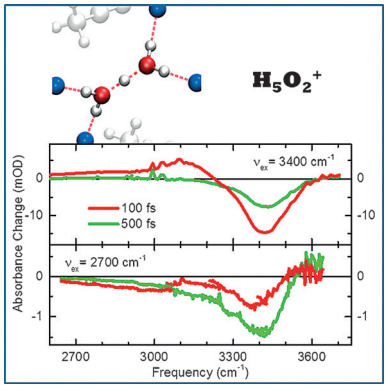


## Femtochemistry



**Partially covered and supported**: An ultrastable gold nanocatalyst was prepared by tuning the strong metal–support interaction between Au nanoparticles (NPs) and a titanium dioxide–hydroxyapatite (HAP) support (see picture). The Au NPs are located at the interfaces of $TiO_2$/HAP support, forming anchored and partially covered active Au NPs.

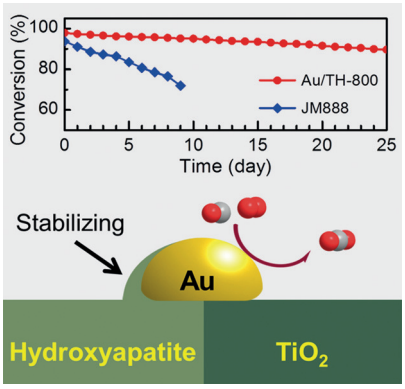


## Metal–Support Interaction



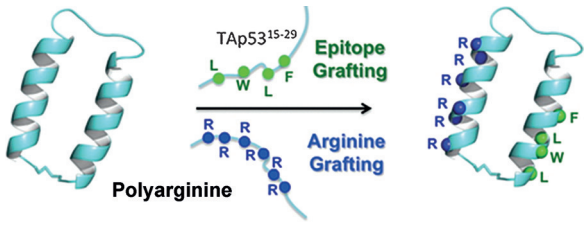


## Therapeutic Peptides



**Hard graft**: A cyclized helix-loop-helix peptide (cyan) was used as a scaffold to generate cell-permeable PPI inhibitors through bifunctional grafting: epitope grafting for binding activity, and arginine grafting for cell permeability. To inhibit p53–HDM2 interactions, the p53 epitope was grafted onto the C-terminal helix and six Arg residues were grafted onto the other helix. The resulting peptide showed cell membrane permeability and inhibitory activity for the intracellular PPI.

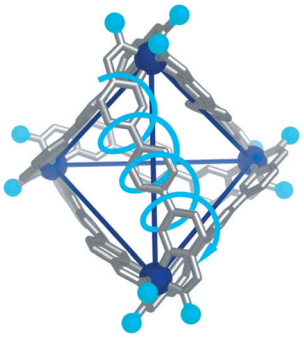

**Powerful coupling**: The derivation and application of a statistical mechanical model to describe stereochemical communication across a range of metal–organic assemblies in terms of intra-vertex and inter-vertex coupling energies is reported. The effect of various structural parameters is thus quantified, allowing for subtle stereochemical outcomes to be predicted.



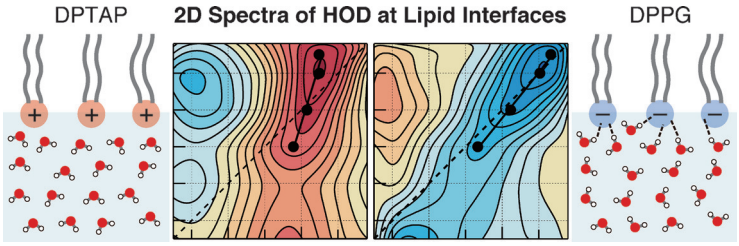


**Femtosecond hydrogen bond fluctuation at lipid membranes**: Interface specific, phase- and time-resolved 2D HD-VSFG spectroscopy, combined with the isotopic dilution technique, has shown that femtosecond water dynamics at lipid interfaces are essentially different, reflecting the chemical structure of the lipid. The observed distinct hydrogen bond fluctuation and dynamics of interfacial water may have a significant influence on cell membrane processes.



**See enzymatic reactions in vivo**: γ-Glu-[1-$^{13}$C]Gly was designed as a hyperpolarized NMR probe for monitoring of GGT activity. The properties of this probe, for example, a large chemical shift change and sufficient hyperpolarization lifetime, are suitable for hyperpolarized $^{13}$C metabolic analysis. The designed probe allowed for the first time the real-time analysis of in vivo GGT activity.

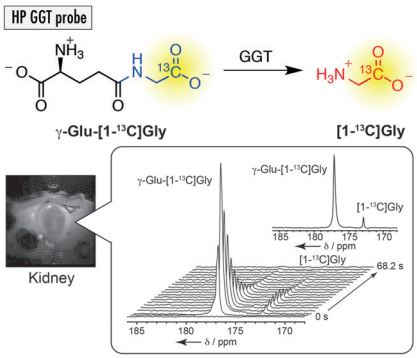




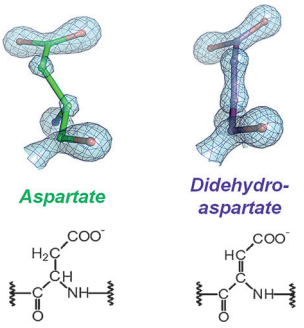


**2H less**: Methyl-coenzyme M reductase catalyzes the reversible reduction of methyl-coenzyme M to methane. Near the active site, it contains the following modified amino acid residues: a thioglycine and four methylated amino acid residues. The presence of a novel post-translationally modified amino acid, didehydroaspartate, adjacent to the thioglycine is revealed by mass spectrometry and high resolution X-ray crystallography.

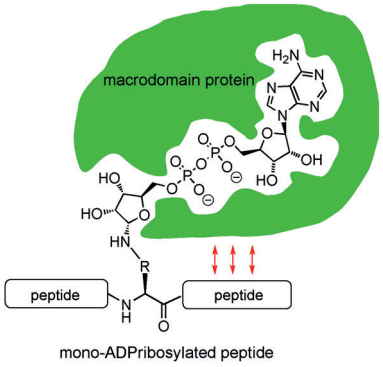


**Ties that bind**: The synthesis of a number of mono-ADP-ribosylated peptides is described. Binding studies of these peptides with different macrodomains showed that the peptide fragment surrounding the ADPr modification influences the binding properties.



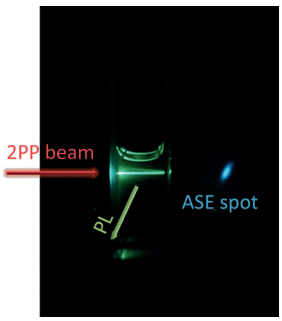


**Highly extended π-conjugated** ladder-type oligo(*p*-phenylene)s containing up to 10 phenyl rings with or without diphenylamino endcaps were synthesized and investigated for their multiphoton absorption properties for blue amplified spontaneous emission (ASE)/lasing. Extremely large two-photon absorption (2PA) cross-sections and highly efficient 2PA ASE/lasing with ultralow threshold were achieved from two-photon pumping (2PP). PL = photoluminescence.



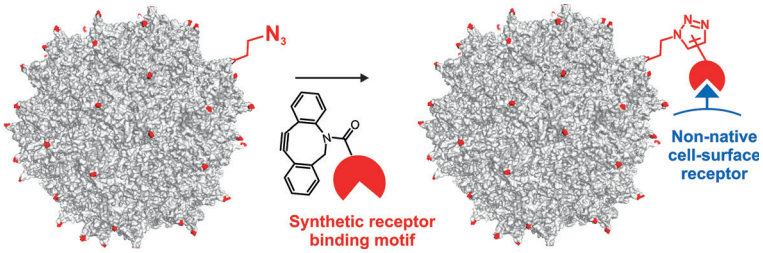


**An adeno-associated virus** (AAV) production platform is reported that enables efficient incorporation of unnatural amino acids into specific sites of the virus capsid. This work provides a general chemical approach to introduce various receptor binding agents onto the AAV capsid with exquisite site selectivity to generate optimized vectors with engineered infectivity.



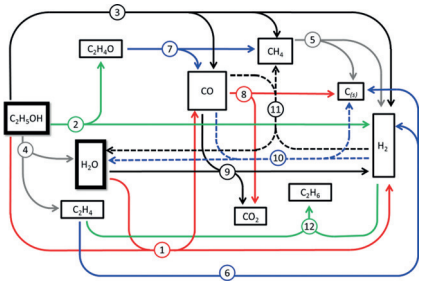


**The tracking of atoms** from reactants to products during Rh/Pt catalytic ethanol steam reforming using $H_3{}^{12}C^{13}CH_2{}^{16}OH$ and $H_2{}^{18}O$ provided new insight into the overall reaction mechanism. All combinations of isotope- and non-isotope-labeled atoms were detected in the products, thus there are multiple pathways involved in $H_2$, CO, $CO_2$, $CH_4$, $C_2H_4$, and $C_2H_6$ product formation.

## Chemical Vapor Deposition



**The critical role** of metastable nanoparticles that are deposited on the substrate during the growth of $MoSe_2$ monolayers in chemical vapor deposition was elucidated. A three-step growth mechanism was proposed to explain their formation and the conversion of these non-stoichiometric nanoparticles into stoichiometric two-dimensional materials.

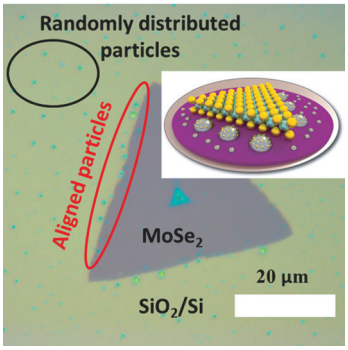


## Electrode Materials



**Mussel power**: A polydopamine-derived material can act as both electrode and binder material for lithium-ion and sodium-ion batteries, and exhibits superior electrochemical performances including high capacity and stable cyclability. The material is synthesized by the oxidative polymerization of dopamine, which is both naturally occurring and biodegradable.

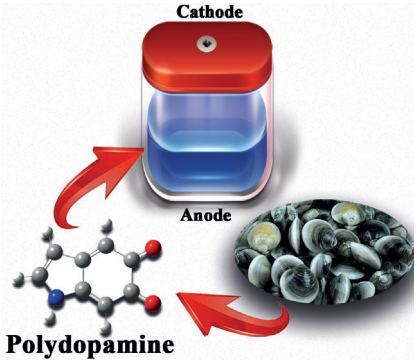


## Proton Conduction



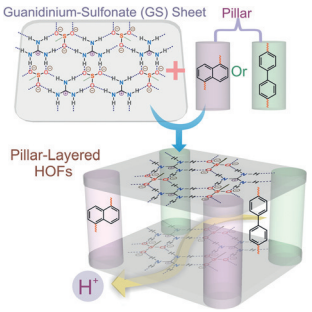


**$H^+$ conduction**: Two porous hydrogen-bonded organic frameworks (HOFs) based on arene sulfonates and guanidinium ions exhibit ultra-high proton conductivity ($\sigma$), $0.75\times10^{-2}$ S cm$^{-1}$ and $1.8\times10^{-2}$ S cm$^{-1}$, under humidified conditions. They also have very low activation energies and higher proton conductivity at ambient conditions compared to other porous crystalline materials, such as MOFs and COFs.

## Organic Thermoelectric Materials



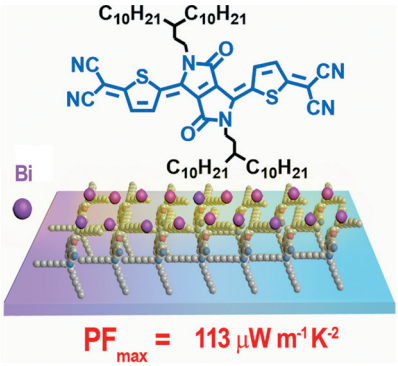


**Interfacial doping for organic thermoelectrics**: Bismuth interfacial doping of thiophene-diketopyrrolopyrrole-based quinoidal molecules results in a maximum power factor ($PF_{max}$) of 113 μW m$^{-1}$ K$^{-2}$. Heavy metal doping of organic semiconductors can open up a new strategy for exploring high performance organic thermoelectric materials.

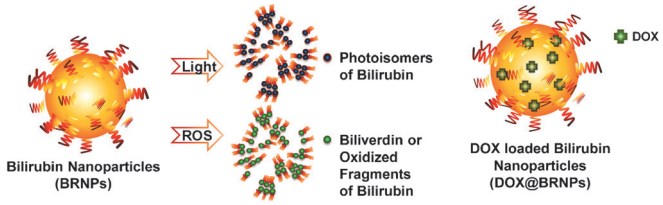


**Aye, there's the rub**: Nanoparticles made of bilirubin, which is an endogenous bioactive bile pigment, show reactive oxygen species (ROS)- and light-responsive particle disruption. Therefore, as well as exerting potent anticancer activity in its own right, bilirubin can be used for the controlled delivery and release of other anticancer drugs, such as doxorubicin (Dox).

## Drug Delivery



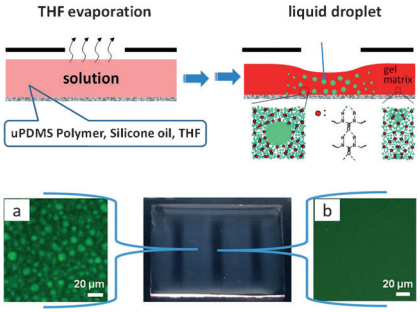


**Evaporative lithography** can be used to control the localization of liquid droplets in a silicone-based polymer matrix. When the solution is placed under a mask, selective solvent evaporation leads to a redistribution of the liquid and polymer components, which results in a patterned film with droplet-containing and droplet-free domains.

## Dynamic Materials



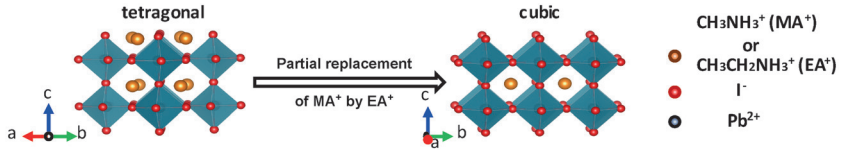


**Despite its large ionic radius**, ethylammonium can partially replace methylammonium in the widely studied 3D hybrid perovskites $CH_3NH_3PbI_3$. This partial replacement results in higher crystal symmetry, improved material stability, and markedly enhanced photocarrier lifetime of the alloy perovskites.

## Hybrid Composites



**It's a wrap**: Sleeve netting provides a cost-effective solution to keep fresh fruits safe and sound. A metal–organic framework (MOF) is used to construct a molecular protective netting on the surface of the rod-like tobacco mosaic virus. The shell thickness was discovered to play a crucial role in the stability of the core–shell composite. More interestingly, the embedded virus particle can be chemically modified using a standard bioconjugation reaction, showing mass transportation within the MOF shell.

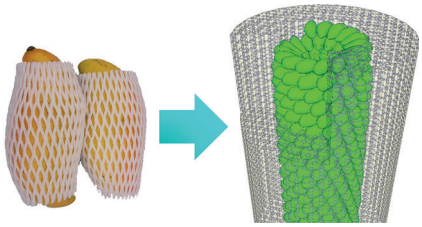

## Metal–Organic Frameworks

## Photochemistry



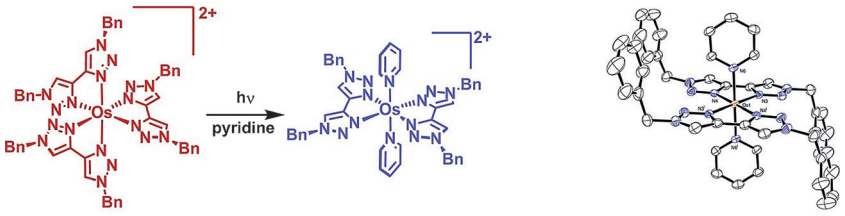


**Defying convention**: The extraordinary ligand ejection photochemistry of the complex $[Os(btz)_3]^{2+}$ in donor solvents is reported along with observation and characterization of both *cis* and *trans* isomers of the ligand-loss intermediate $[Os(\kappa^2\text{-btz})_2(\kappa^1\text{-btz})(NCMe)]^{2+}$ (btz = 1,1′-dibenzyl-4,4′-bi-1,2,3-triazolyl).

## Mesoporous Materials



**Pores for thought**: The assembly of silica nanospheres of different sizes into a binary colloidal crystal has resulted in a superlattice of nanospace. The CrB-type binary silica colloidal crystals contain interstitial mesopores of different sizes that are spatially separated along the stacking direction. An oriented thin film of the binary nanoparticle mesoporous superlattice has been fabricated on a silicon substrate by dip coating.

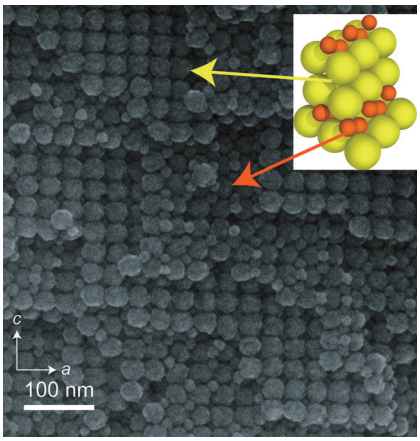


## Organic 2D Materials



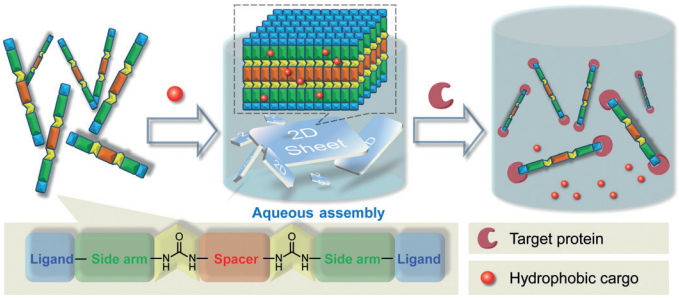


**Special assemblies** of small organic molecules form nano/microscale supramolecular 2D materials in aqueous media. These assemblies can be programmed to disassemble in response to a protein and release their non-covalently bound guest molecules.

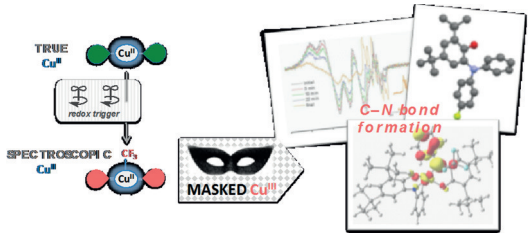


**$Cu^{III}$ in hiding**: A stable copper(II) complex bearing fully oxidized iminobenzoquinone redox ligands reacts as a copper(III) species and performs high-yielding C–N bond formation. Mechanistic studies suggest that this behavior could stem from a mechanism akin to reductive elimination occurring at the metal center but facilitated by the ligand.



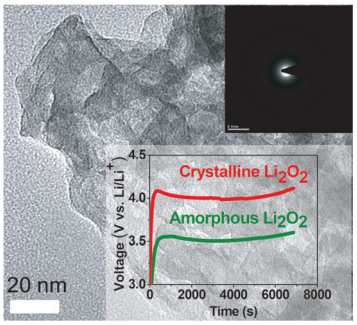


**Better off amorphous**: Amorphous $Li_2O_2$ has been synthesized by a rapid reaction of $TMAO_2$ and $LiClO_4$ in solution, and its amorphous nature has been confirmed by a range of techniques. Compared with its crystalline siblings, amorphous $Li_2O_2$ demonstrates increased charge-transport capabilities and enhanced oxidation kinetics, manifesting itself a desirable discharge phase for high-performance $Li–O_2$ batteries.



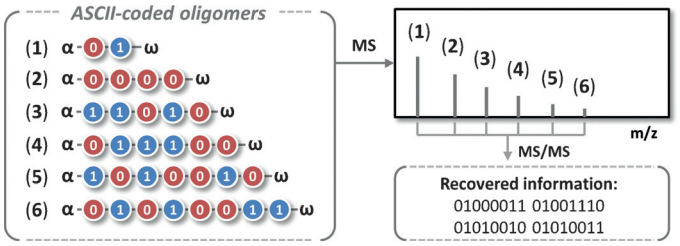


**Mass-produced encryption**: Mixtures of monodisperse sequence-coded oligomers of different length were studied by tandem mass spectrometry. These "intentionally polydisperse" mixtures allow storage of a substantial amount of molecular information that can be rapidly deciphered.



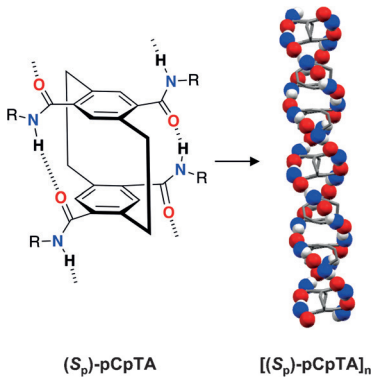


**Laced up**: [2.2]Paracyclophane (pCp) derivatives are capable of programmed self-assembly into extended cofacial π-stacks in solution and in the solid state. The one-dimensional arrangements are homochiral and helically laced-up by a combination of transannular (intramolecular) and intermolecular hydrogen bonds. pCpTA = pCp-4,7,12,15-tetracarboxamide.

## Biofilms



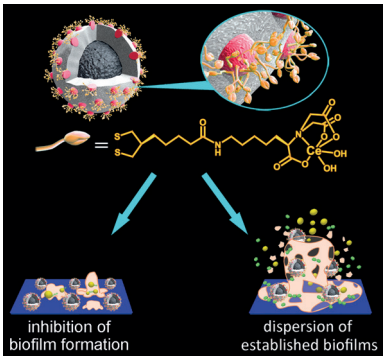


**An artificial enzyme** for DNA cleavage was obtained by confining protected gold nanoparticles with multiple $Ce^{IV}$ centers on colloidal magnetic $Fe_3O_4/SiO_2$ core/shell particles. This system efficiently inhibited the formation of biofilms, dispersed preformed films, and enabled the eradication of biofilms when used in combination with common antibiotics.

## Supramolecular Catalysis



**Hop on, hop off**: Metal ions are reversibly released from an electrode to regulate the activity of a gold nanoparticle catalyst (see picture). The system catalyzes the cleavage of 2-hydroxypropyl-*p*-nitrophenyl phosphate and the formation of *p*-nitrophenolate can be monitored by UV/Vis spectroscopy.

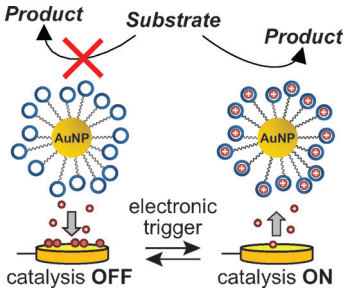


## Protein Ionization



**Multiple ionization**: Exposure of gas-phase ubiquitin ions to intense femtosecond pulses from an extreme ultraviolet free-electron laser leads to almost simultaneous removal of many electrons. Before the deposited excitation energy equilibrates, localized fragmentation processes at the ionization sites predominantly lead to formation of immonium ions.

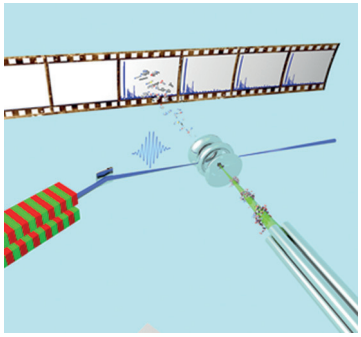

## NMR Spectroscopy



**Directing polarization**: By using a biradical-labeled ligand, dynamic nuclear polarization (DNP) can be efficiently and very specifically directed to a target protein. This behavior makes it possible to filter out the signal of the target protein from a large background (see picture), enabling a selective solid-state NMR characterization in increasingly native environments such as found in crude cell lysates.

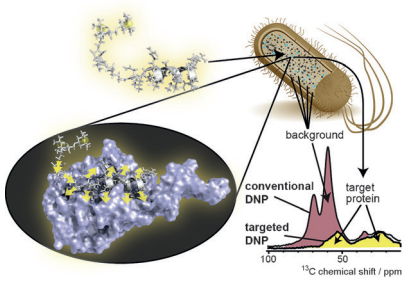

**Hydrogenated graphene** was functionalized through a dehydrogenative cross-coupling reaction between an allylic C–H bond on the graphene material and an α-C–H bond of tetrahydrothiophen-3-one. The functionalized hydrogenated graphene material benefits from improved dispersion stability in water.

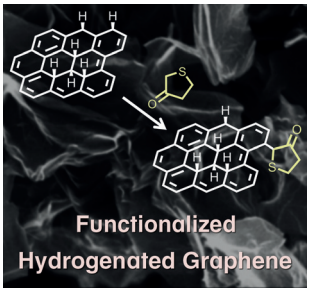




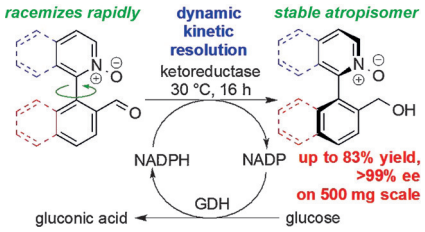


**Speedy resolution**: Enzymatic reduction of rapidly racemizing biaryl aldehydes yields, by highly selective dynamic kinetic resolution (DKR), single enantiomers of atropisomeric biaryls in high yield and with high *ee* values. This first atropselective enzymatic DKR gives products that contain a pyridine N-oxide and primary alcohol groups and function as catalysts of asymmetric aldehyde allylation.



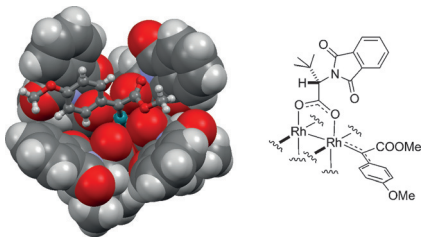


**Avec des "Si" on refait le monde**: The *Si*-face of a chiral push/pull dirhodium carbene has been shown to be open to attack by an incoming partner (e.g. styrene) when $[Rh_2\{(S)\text{-PTTL}\}_4]$ (PTTL = *N*-phthaloyl-*tert*-leucinate) is used as a precatalyst. The shape of the chiral binding site is primarily defined by the conformational preferences of the chiral ancillary ligands and reinforced by a network of weak interligand interactions.



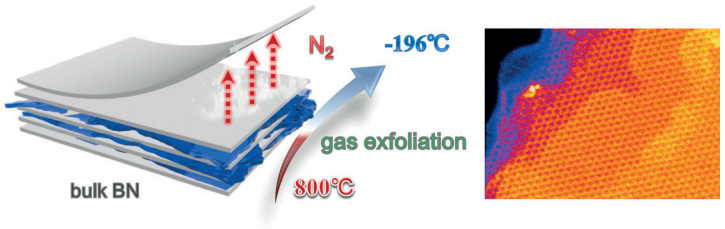


**Layered structures**: A novel and efficient thermal-expansion-triggered gas exfoliation of boron nitride into few-layered nanosheets was successfully developed (see picture). This method can also be used to produce other layered materials in high yields.

## Plasmonic Nanostructures



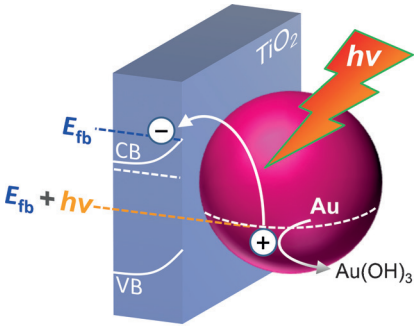


**Plasmonic photooxidation ability**: The anodic photopotential of plasmon-induced charge separation was evaluated on the basis of surface hydroxylation of gold nanoparticles deposited on $TiO_2$. It was found that the potential is determined by the flat band potential of $TiO_2$ ($E_{fb}$), which depends on the electrolyte pH, and irradiated photon energy ($h\nu$).

## Metal–Organic Frameworks



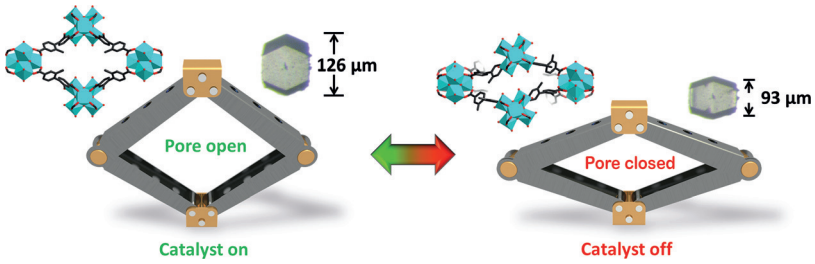


**An open and shut case**: The inherent cavities and dynamic behavior of flexible MOFs, bear a close resemblance to regulatory enzymes. Switchable activation and deactivation of their catalytic properties occurs on pore opening and closing by solvation/solvent removal.

## Halogenation



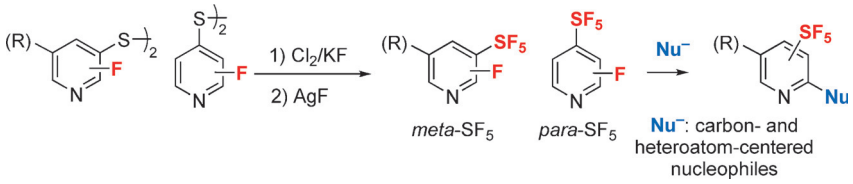


**It had to be you...** A general route for the synthesis of *m*- and *p*-$SF_5$-substituted pyridines is disclosed. The fundamental synthetic sequence is the same as those reported for *ortho*-$SF_5$-substituted pyridines and $SF_5$-substituted arenes. In this case, however, at least one fluorine atom on the pyridine ring is essential for the success of the transformation. The fluorine substituent can later be substituted by a C, N, O, or S nucleophile (see scheme).

## $^{18}$F-Fluorination



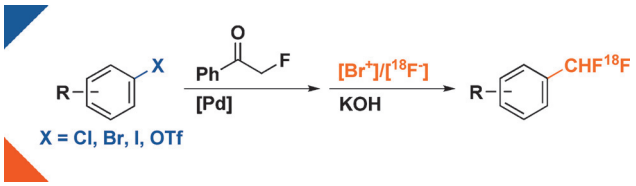


**PET peeve resolved**: A general method for the synthesis of $[^{18}F]CHF_2$-arenes from $[^{18}F]$fluoride enables labeling of a variety of arenes and heteroarenes with radiochemical yields (not decay-corrected) from 10 to 60%. The $^{18}$F-fluorination precursors are readily prepared from aryl chlorides, bromides, iodides, and triflates. Seven $^{18}$F-difluoromethylarene drug analogues and radiopharmaceuticals were synthesized to show the potential of the method.

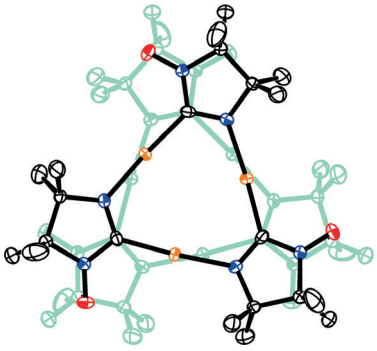

**Triangulation**: An open-shell iminonitroxide/gold(I) trimer complex was prepared. The intramolecular exchange interaction between the iminonitroxide moieties was found to be positive ($J_{intra}/k_B \approx +29$ K). This quartet iminonitroxide/gold complex produced an intercalated silver(I) complex with a ferromagnetic interaction ($J_{intra}/k_B \approx +25$ K) for the trimer unit.

## Magnetic Properties



**All rolled into one**: Liquid marbles based on magnetic upconversion nanoparticles (UCNPs) exhibit excellent magnetic and mechanical properties and were used for the conversion of low-energy near-infrared photons into high-energy UV/Vis photons. They might find application in photodynamic therapy as well as for magnetically controlled drug delivery and release and multifunctional actuation.

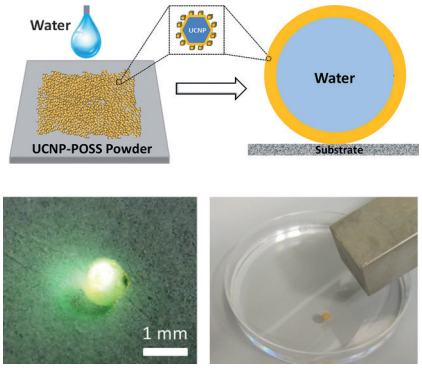


## Photodynamic Therapy



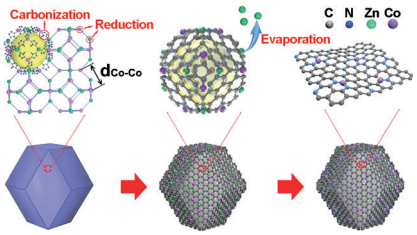


**Singles Club**: A general strategy enabling the practical and controlled synthesis of supported metal single-atom catalysts with atomic dispersion, high metal loading, and excellent molecular accessibility has been developed and applied to a series of metal single atoms supported on N-doped carbon.

## Single-Atom Catalysis



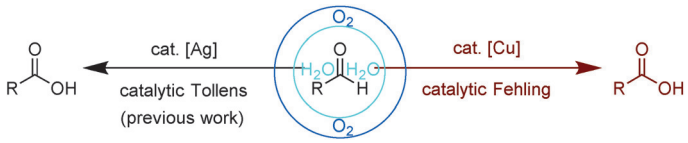


**Without 'Fehl'**: The first example of homogeneous copper-catalyzed aerobic oxidation of aldehydes is reported. This method utilizes atmospheric oxygen as the sole oxidant, proceeds under extremely mild aqueous conditions, and covers a wide range of various functionalized aldehydes. Chromatography is generally not necessary for product purification.

## Oxidation

## Sulfoxidation



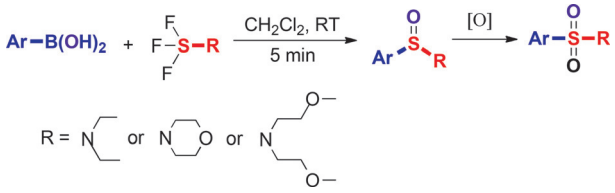


**Mighty mild**: A wide range of arylboronic acids and their derivatives underwent efficient cross-coupling under mild and metal-free conditions with reagents based on the electrophilic fluorination reagent diethylaminosulfur trifluoride (DAST). This simple and convenient method directly afforded sulfinamides, which could be further converted into sulfonamides through a straightforward oxidation step (see scheme).

## Asymmetric Catalysis



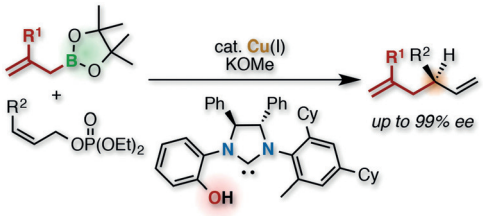


**Novel NHC**: Copper-catalyzed enantioselective allyl–allyl couplings between allylboronates and either *Z*-acyclic or cyclic allylic phosphates are accomplished by using a new chiral NHC ligand bearing a phenolic hydroxy group. This reaction occurs with exceptional $S_N2'$-type regioselectivities to deliver chiral 1,5-dienes with a tertiary stereogenic center at the allylic/homoallylic position.

## Synthetic Methods




**Expanding the scope**: An efficient and metal-free approach for the elusive azidocyanation of unactivated alkenes is proposed. The strategy of intramolecular distal cyano migration is combined with alkene difunctionalization for the first time. A variety of useful azido-substituted alkyl nitriles are readily prepared in good yields and with exquisite regio- and stereoselectivities.

## Asymmetric Catalysis




**The third pillar**: The intrinsic limitation of asymmetric Mannich reactions—their failure with imine substrates containing a primary alkyl substituent—was solved by employing dithiomalonates as Mannich donors and a chiral squaramide organocatalyst. This protocol was used to develop a concise organocatalytic, coupling-reagent-free synthesis of the antidiabetic drug (−)-(*R*)-sitagliptin (see scheme).

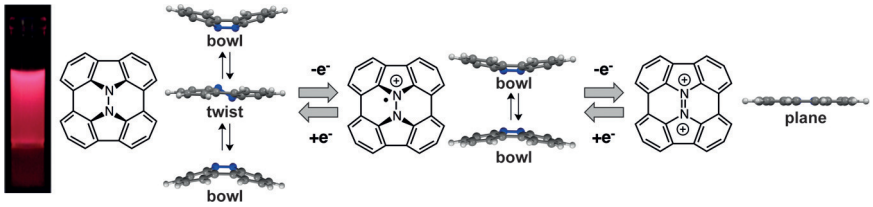


**Behavior to bowl you over**: A red-fluorescent heterobuckybowl—a heteroatom-containing partial bowl structure of fullerene—was synthesized that had bowl and twist structures in the neutral state, a shallow bowl structure in the monocation state, and a planar structure in the dication state. A reversible transformation from the curved bowl/twist shape to the planar shape was found to occur upon two-electron oxidation (see picture).

## Heterobuckybowls



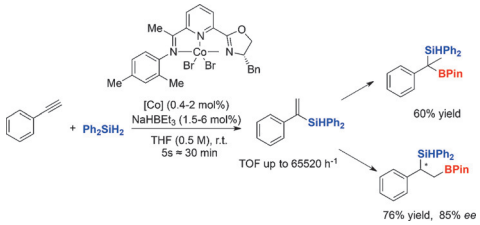


**Cobalt catalysis**: A highly chemo-, regio- and stereoselective cobalt-catalyzed hydrosilylation reaction of alkynes with silanes was developed (see picture; HBPin = pinacol borane; TOF = turnover frequency). The reaction tolerates various functionalized groups, which may lead to further applications and late-stage derivatizations.

## Hydrosilylation of Alkynes



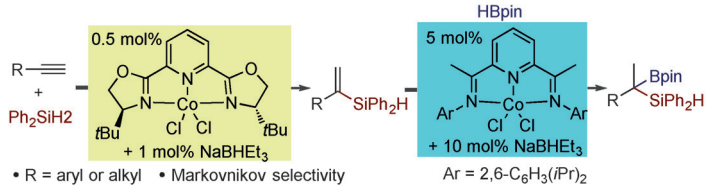


**Terminal alkynes** can be converted into α-vinylsilanes in a cobalt-catalyzed Markovnikov alkyne hydrosilylation reaction with $Ph_2SiH_2$. The reaction products were further transformed into novel geminal borosilanes in a cobalt-catalyzed hydroboration process, also with Markovnikov selectivity.

## Vinylsilanes



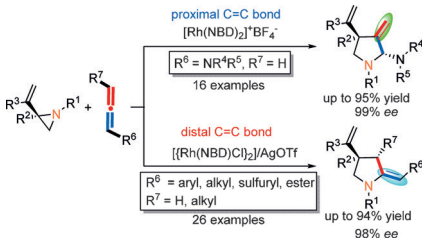


**Adding together rapidly**: A regiodivergent synthesis of enantioenriched functionalized pyrrolidines, such as 2-methylene- and 3-methylene-pyrrolidines, has been developed through a regioselective [3+2] cycloaddition of vinyl aziridines with allenes and N-alleneamines, respectively. The reaction demonstrates general substrate scope, mild conditions, atom-economy, and proceeds with complete chirality transfer.

## Heterocycles



  

**Chemical twins**: The subnitridometalates $Ba_{23}Na_{11}(MN_4)_4$ (M = V, Nb, or Ta) can be described as "chemical twins" with separated ionic and metallic motifs. The chemistry of the subnitrides was thus extended through the incorporation of complex nitridometalate anions into a metallic matrix of barium and sodium atoms.

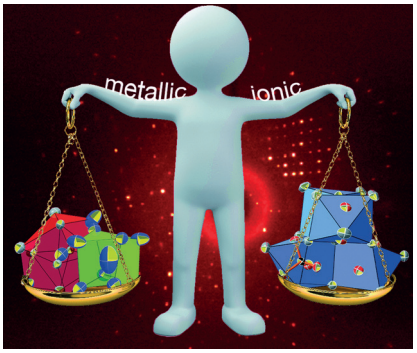


## Subnitridometalates



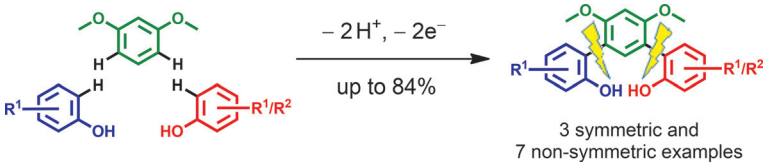


**Two selective couplings** enable the generation of *meta*-terphenyl-2,2″-diols in a metal- and reagent-free manner in an electrosynthetic process. The reactions are scalable and very simple to perform and provide access to precursors for pincer ligands.

## Electrosynthesis



**Give me an O**: Mass spectrometry studies and quantum chemical calculations show that the selective oxidation of methane to methanol promoted by $[AuO]^+$ proceeds by oxygen-atom transfer. The signal labeled with "x" is due to reactions with background contaminants.

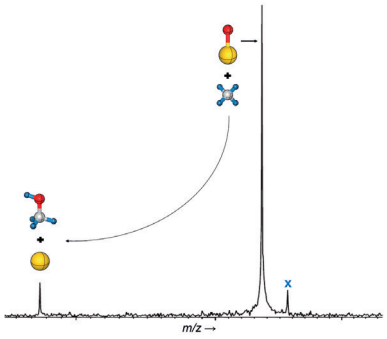


## Gas-Phase Reactions



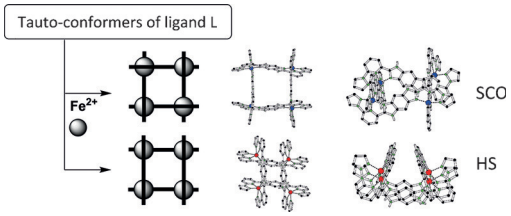


**The coordination** of $Fe^{II}$ metal ions by a homoditopic ligand **L** with two tridentate chelates leads to the tautomerism-driven emergence of complexity. The two tautoisomeric $Fe^{II}_4L_4$ tetramers that were thus formed exhibit different magnetic properties. One complex undergoes spin crossover (SCO), whereas the other one is blocked in the $Fe^{II}$ high spin (HS) state.

## Iron(II) Complexes

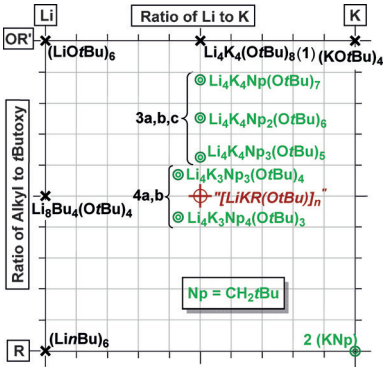


**Bases à la carte**: A reaction of neopentyllithium ($LiCH_2tBu$) with potassium *tert*-butoxide (KO*t*Bu) forms alkane-soluble mixed alkyl/alkoxy aggregates containing both lithium and potassium ions. These neopentyl analogues of the Lochmann–Schlosser superbase are products with varying compositions $Li_xK_yNp_z(OtBu)_{x+y-z}$ (see Scheme), the outcome of a complicated equilibrium based on the concentration and solubilities of its components.



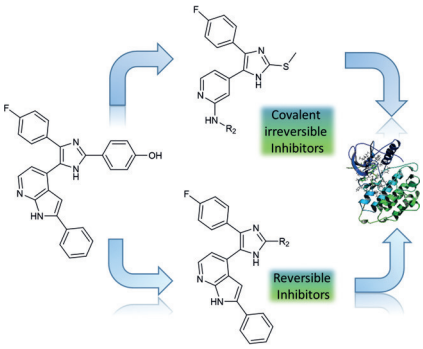


**From reversible to irreversible and back**: A new class of trisubstituted imidazoles (see scheme) was designed to overcome drug resistance caused by the EGFR mutation T790M in non-small-cell lung cancer, predominantly through non-covalent interactions. In contrast to third-generation irreversible EGFR inhibitors, these imidazoles are up to 350-fold less vulnerable to Cys 797 mutation and show high cellular activity in the low double-digit nanomolar range.



A dual-phase ceramic membrane consisting of 50 mol% $BaCe_{0.85}Fe_{0.15}O_{3-\delta}$ and 50 mol% $BaCe_{0.15}Fe_{0.85}O_{3-\delta}$ is formed automatically by demixing of $BaCe_{0.5}Fe_{0.5}O_{3-\delta}$ through calcination. The first perovskite phase acts as the main proton conductor and the other as the main electron conductor. The composite ceramic shows an extremely high $H_2$ permeation flux. This concept can also be used for the synthesis of other ceramics.

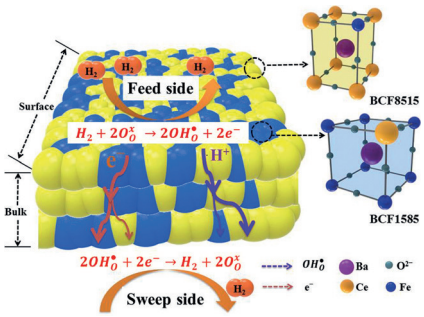




**A feather in your cap**: A straightforward approach is presented for the efficient production of a range of *N*7-modified 5′-caps on mRNAs based on the highly promiscuous methyltransferase Ecm1. These can be used to tune translation of the respective mRNAs both in vitro and in cells. Appropriate modifications allow subsequent bioorthogonal reactions, as demonstrated by intracellular live-cell labeling of a target mRNA.

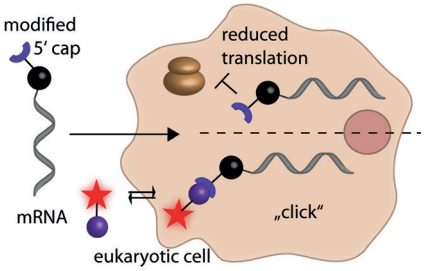

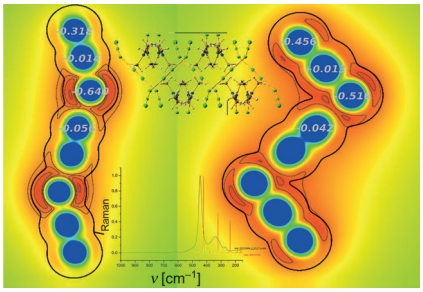


**Being discrete**: The new polychloride salt $[CCl(NMe_2)_2]^+_2[Cl_8]^{2-}$ (tetramethylchloroamidinium octachloride) was crystallized from an ionic liquid and fully characterized. It is the first dianion of a polychloride to be reported. Detailed quantum-chemical calculations show the salt is made up of discrete $[Cl_8]^{2-}$ anions which do not show any tendency to build up networks through halogen bonding.

## Polychlorides



**Methods against mutants**: Targeting acquired drug resistance represents the major challenge in the treatment of EGFR-driven non-small-cell lung cancer. Complex crystal structures of new covalent inhibitors and detailed kinetic studies provide insight into the key features required for targeting EGFR mutations, including EGFR-L858R/T790M/C797S.

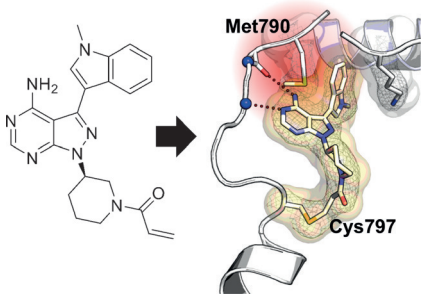


## Enzyme Inhibitors



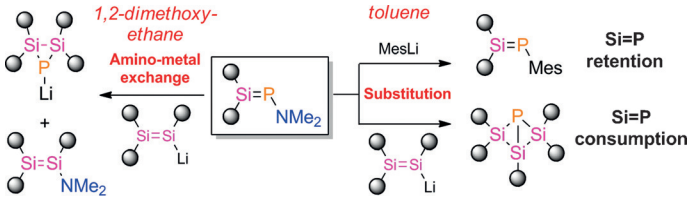


**The $NMe_2$ group as a leaving group on the P=Si bond**: An electrophilic phosphasilene reacts with MesLi under substitution and retention of the double bond. With $Tip_2Si{=}Si(Tip)Li$ (Tip = 2,4,6-*i*$Pr_3C_6H_2$) the Si=P bond is consumed after initial substitution to yield a trisilaphospha-[1.1.0]bicyclobutane. In contrast, in the donor solvent dme, an amino–metal exchange occurs.

## Main-Group Chemistry



Supporting information is available on www.angewandte.org (see article for access details).

A video clip is available as Supporting Information on www.angewandte.org (see article for access details).

This article is available online free of charge (Open Access).

This article is accompanied by a cover picture (front or back cover, and inside or outside).

The Very Important Papers, marked VIP, have been rated unanimously as very important by the referees.

The Hot Papers are articles that the Editors have chosen on the basis of the referee reports to be of particular importance for an intensely studied area of research.

# Angewandte Corrigendum

## Water-Assisted Nitrile Oxide Cycloadditions: Synthesis of Isoxazoles and Stereoselective Syntheses of Isoxazolines and 1,2,4-Oxadiazoles

C. Kesornpun, T. Aree, C. Mahidol, S. Ruchirawat, P. Kittakoop* ——— **3997–4001**

*Angew. Chem. Int. Ed.* **2016**, *55*

DOI: 10.1002/anie.201511730

In this Communication, the following mistakes need to be corrected:
Page 3997: The sentence "Therefore, the synthesis of isoxazolines and isoxazoles is carried out in solvents containing bases as catalysts" should be corrected as "Therefore, the synthesis of isoxazolines and isoxazoles is carried out in solvents containing bases."
The minor regioisomer of individual isoxazolines shown in Scheme 2 and Figure 2S (Supporting Information) and isoxazoles displayed in Scheme 5 and Figure 5S might be present in the crude products; details of regioisomers of some compounds were previously reported by Huisgen and co-workers.[1]
Page 3999: The claim that "the preparation of the novel hybrid isoxazoline-oxadiazoles presented here has never been reported" is wrong. The hybrid isoxazoline-oxadiazole was previously reported by Bettinetti and Gamba in 1970.[2] However, the spectroscopic and crystallographic determination of the stereochemistry of this compound class has been successfully established in the current work.
Page 3999: "... converted into (bis)**6bo** during crystallization, and it has a plane of symmetry (*meso* form)". The optical rotation of (bis)**6bo** that was incorrectly measured to a close-to-zero value led to the wrong conclusion that (bis)**6bo** has *meso* form. The correct optical rotation of (bis)**6bo** is −289.0 ($c = 0.42$ in DMSO). Moreover, after examining X-ray crystallographic data, it was found that (bis)**6bo** has a pseudo-twofold axis through the bridge oxygen atom; therefore it is a chiral molecule.
Page 4000: In Scheme 5, the structure of **8dh** needs to be revised as shown below.

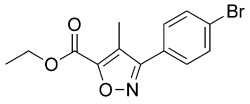

Previously proposed structure of **8dh**

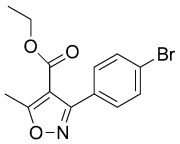

The correct structure of **8dh**

The authors sincerely apologize for these errors. They are grateful to Prof. Manfred Christl, University of Würzburg, for helpful comments.

[1] a) K. Bast, M. Christl, R. Huisgen, W. Mack, R. Sustmann, *Chem. Ber.* **1973**, *106*, 3258–3274; b) K. Bast, M. Christl, R. Huisgen, W. Mack, *Chem. Ber.* **1972**, *105*, 2825–2840; c) M. Christl, R. Huisgen, *Chem. Ber.* **1973**, *106*, 3345–3367; d) M. Christl, R. Huisgen, R. Sustmann, *Chem. Ber.* **1973**, *106*, 3275–3290.
[2] G. F. Bettinetti, A. Gamba, *Gazz. Chim. Ital.* **1970**, *100*, 1144–1159.

# Angewandte Corrigendum

## A Click Chemistry-Based Proteomic Approach Reveals that 1,2,4-Trioxolane and Artemisinin Antimalarials Share a Common Protein Alkylation Profile

H. M. Ismail, V. E. Barton, M. Panchana, S. Charoensutthivarakul, G. A. Biagini, S. A. Ward, P. M. O'Neill* — **6401–6405**

*Angew. Chem. Int. Ed.* **2016**, *55*

DOI: 10.1002/anie.201512062

In this Communication there was an error in the structures of negative controls CP1 (**6b**) and CP2 (**7b**) (Figures 2 and 3) and intermediate **10** (Scheme 2). The correct structures are given below.

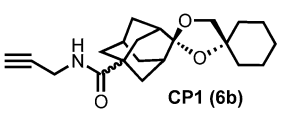

CP1 (6b)

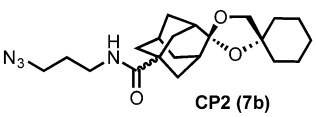

CP2 (7b)

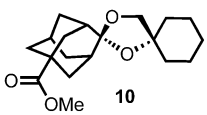

10

These errors have no bearing on the conclusions reached in the manuscript. The authors apologize for these errors.

  

# Angewandte Corrigendum

In Figure 2c of this Communication, the label on the horizontal axis was wrongly given as "*t*/h" instead of "*t*/min". The correct version of Figure 2c is given below. The authors apologize for this mistake.

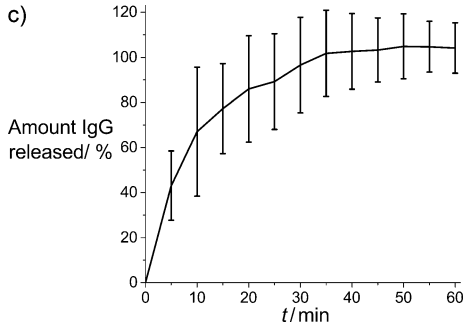


***Figure 2.*** [...] c) Release of fluorescence-labeled IgG antibodies from hydrogel beads (10 mg mL$^{-1}$).

Noncovalent Hydrogel Beads as Microcarriers for Cell Culture

R. Wieduwild, S. Krishnan, K. Chwalek, A. Boden, M. Nowak, D. Drechsel, C. Werner,* Y. Zhang* —— **3962–3966**

*Angew. Chem. Int. Ed.* **2015**, *54*

DOI: 10.1002/anie.201411400



  